

## On the low-lying Rydberg states of azabenzenes

C. F. Dion and E. R. Bernstein

Citation: *The Journal of Chemical Physics* **103**, 4907 (1995); doi: 10.1063/1.470626

View online: <http://dx.doi.org/10.1063/1.470626>

View Table of Contents: <http://aip.scitation.org/toc/jcp/103/12>

Published by the *American Institute of Physics*

---

---

**COMPLETELY**

**REDESIGNED!**



**PHYSICS  
TODAY**

*Physics Today* Buyer's Guide  
Search with a purpose.

# On the low-lying Rydberg states of azabenzene

C. F. Dion and E. R. Bernstein

Department of Chemistry, Colorado State University, Fort Collins, Colorado 80523

(Received 11 April 1995; accepted 26 June 1995)

Mass resolved excitation spectra of supersonic expansion cooled mono- and diazabenzene are reported for the low lying Rydberg states. Transitions are located for pyridine, pyrazine, and pyridazine, but not pyrimidine. The Rydberg state lifetimes of these molecules are estimated, based on a Lorentzian line shape analysis, to be ca. 500 fs. *Ab initio* calculations for pyrazine at the complete active space self-consistent-field (CASSCF) and CASSCF many-body second-order perturbation theory (CASSCF/MBPT2) levels show that extensive configuration interaction and dynamic electron correlation are necessary to account for the excited states of these systems. © 1995 American Institute of Physics.

## I. INTRODUCTION

The high energy states of molecules play an important role in their chemical and physical properties. In particular, Rydberg states (those with principle quantum number greater than the valence state's principle quantum number— $n > 2$  for organic systems) have been implicated in ionization processes,<sup>1</sup> energetic material ignition chemistry,<sup>2</sup> photodissociation chemistry,<sup>3</sup> and enhanced excited state reactivity.<sup>4</sup> The lower energy Rydberg states of molecules are often thought to be localized on a particular atom, especially for molecules with heteroatoms such as nitrogen and oxygen.<sup>5</sup> Transitions to such Rydberg states are often characterized by the atomic-like description  $3s2p \leftarrow (2p)^2$ ,  $3p2p \leftarrow (2p)^2$ , etc. or  $3s\sigma \leftarrow (\sigma)^2$ , etc. Examples of such modeling can be found for simple amines,<sup>5</sup> ethers,<sup>6</sup> and even hydrocarbons.<sup>7</sup> In the past few years we have studied the low lying Rydberg transitions of azabicyclooctanes (ABCO and DABCO),<sup>3,4</sup> methyl and ethyl amines,<sup>8</sup> hexamethylenetetramine (HMT),<sup>4</sup> dioxane,<sup>9</sup> methyl, ethyl, and vinyl ethers,<sup>6</sup> and adamantane.<sup>7</sup> This effort includes both experimental and theoretical studies. One of the main results of these investigations is that molecular Rydberg states are not localized states on a single atom, and indeed, they can be quite complex with regard to electronic distribution. Evidence for this more complex model of Rydberg state behavior and characterization comes from three different, but complementary, sources: (1) detailed spectroscopic data for isolated molecules which show molecular vibronic structure related to motion of "distant" groups (e.g., methyl rotor motion, etc.);<sup>5(b),10</sup> (2) resolved cluster spectra which evidence solvent shifts for Rydberg states that are a function of solvent coordination site on the chromophore;<sup>4,9</sup> and (3) high level (e.g., CASSCF/MP2) *ab initio* ground and excited state calculations for amines.<sup>11</sup>

The study of Rydberg states of amines has had a long history.<sup>5,11</sup> Ammonia is certainly a well-studied system and its first three excited electronic states are Rydberg ( $3s, 3p, 3p$ ) states.<sup>5</sup> We have recently studied methyl and ethyl substituted ammonia<sup>8</sup> and have been able to identify two electronic states, one of which is a Rydberg state.<sup>8</sup>

All the above-mentioned studies have been carried out employing the now familiar technique of supersonic jet, mass-resolved spectroscopy rather than static gas phase

absorption.<sup>3,9,12</sup> The advantage of absorption techniques is that broad transitions can be detected, in particular short-lived states<sup>13</sup> or species are quite accessible. The advantage of the supersonic jet "secondary" or "trigger" detection techniques (e.g., fluorescence excitation, ion or electron detection) is that longer-lived ( $\geq 10$  ps, for ns pulsed lasers) states that are well resolved (like Rydberg states) can be selectively accessed. Absorption detection for static gas phase samples of monocyclic amines (e.g., piperazine, piperidine, etc.) has located apparent broad Rydberg transitions for piperidine ( $C_5H_{10}N$ ) and piperazine ( $C_4H_8N_2$ ) but no sharp features are observed for these monocyclic amines in a supersonic jet/fluorescence or mass spectrometer detection apparatus.<sup>14</sup> This is a somewhat surprising result which suggests that a systematic understanding of molecular amine Rydberg states is not presently available. Indeed, the motivations behind the present effort are summarized as follows: to learn more about the Rydberg states of aromatic amines especially in the presence of other overlapping transitions; to learn more about the localization/delocalization of amine Rydberg states; to elucidate and understand how Rydberg states relax and decay; and to elucidate how amine Rydberg states interact (and react) with other species.

In this report we discuss the azabenzene series pyridine, pyrazine, pyrimidine, and pyridazine with regard to its set of low lying  $3s/3p$  Rydberg states. We have remeasured these transitions under extreme cooling, supersonic jet conditions in order to study origins, linewidths, vibronic features and possible rotational structure. Additionally, *ab initio* calculations are presented for pyrazine to help understand the electronic transitions observed in terms of electron distributions in the molecules and to explore further the requirements necessary for accurate *ab initio* transition energies in these systems.

Experimental studies of azabenzene have been reviewed previously,<sup>15</sup> but the main focus of these reviews has not been the Rydberg states. Nonetheless, the Rydberg states are included and one can learn a good deal about them from comments in these references. The  $2p3s$  ( $^1A_1$ ) Rydberg state of pyridine has been assigned to lie at  $50\,670\text{ cm}^{-1}$  with  $1^1=982$  and  $6a^1=598\text{ cm}^{-1}$ . A  $3p$  Rydberg state is suggested at  $55\,250\text{ cm}^{-1}$ . The two lowest lying Rydberg states of pyridazine are suggested to lie at  $47\,565\text{ cm}^{-1}$  ( $2p3s$ )<sup>16</sup>

and ca.  $51\,000\text{ cm}^{-1}$  ( $2p3p$ ).<sup>15</sup> Neither of these features is found in this study, in any relevant mass channel. A feature assigned as a triplet state for pyridazine<sup>15</sup> is observed in this study ( $53\,313\text{ cm}^{-1}$ ) and may well be the first singlet  $2p3p$  Rydberg state. The Rydberg states of pyrimidine are reported to lie at  $51\,124\text{ cm}^{-1}$  ( $2p3s, {}^1B_2$ ) and possibly a ( $2p3p$ ) state at  $56\,271\text{ cm}^{-1}$ , but are not observed in the present study. Pyrazine Rydberg states are reported at  $50\,699\text{ cm}^{-1}$  ( $2p3s, A_{1g}$ ) and tentatively at ca.  $55\,000\text{ cm}^{-1}$  ( $2p3p, {}^1B_{3u}, {}^1B_{2u}, B_{1u}$ ).

None of the previous studies are carried out for supersonic jet cooled samples with mass-resolved detection. Our motivations behind such experiments are confirmation of the assignments, linewidth and shape determinations, and identification of additional vibronic features.

The experimental studies reported in this work are supersonic jet mass-resolved spectroscopy of the mono- and diazines pyridine, pyridazine, pyrimidine, and pyrazine. The transitions are observed by two photon absorptions to the Rydberg state with an additional photon from the same laser to ionize the excited molecule (i.e., a 2+1-resonance-enhanced ionization). For azabenzenes of  $C_{2v}$  symmetry (see Ref. 15 for axes) two photon transitions are allowed from the  $A_1$  ground state to all excited electronic states without vibronic assistance. Purely electronic two-photon transitions in pyrazine ( $D_{2h}$  symmetry) occur between the  $A_g$  ground state and all excited states of  $g$  symmetry.

Additionally, a number of theoretical *ab initio* studies of azabenzenes have also appeared, with particular attention paid to pyrazine.<sup>17–20</sup> Since the work of Goddard *et al.*<sup>17</sup> the model of interacting localized excitation on the nitrogen atoms of diazabenzenes has been the accepted one for the description of the excited  $n\pi^*$  and  $\pi\pi^*$  states. This model can be incorporated into a generalized valence bond approach<sup>17</sup> or can be effectively achieved within a complete active space self-consistent-field (CASSCF) multireference configuration interaction (MRCI) approach with second-order many-body perturbation theory (MBPT2)<sup>21–23</sup> accounting for the remaining dynamic electron correlation. This latter approach has been applied to a number of systems, including the azabenzene  $n\pi^*$  and  $\pi\pi^*$  excitations.<sup>21</sup> A concomitant reduction in the wave-function symmetry from  $D_{2h}$  to  $C_{2v}$  for pyrazine occurs with this “localization” and increased configuration interaction. Given these important augmentations to the usual multiconfiguration CASSCF theory, a major fraction of the dynamic electron correlation can be accounted for and reasonable agreement between theory and experiment can be achieved for  $n\pi^*$  and  $\pi\pi^*$  excited states.<sup>20</sup> If a large enough multireference configuration interaction calculation (MRCI) could be employed for the azines, the approach would, in principle, be effective as well. Other calculations on azabenzenes<sup>20,24,25</sup> have been reported involving extensive CI and MRCI algorithms with good results for  $n\pi^*$  and  $\pi\pi^*$  states. All methods point to the conclusion that extensive CI is an essential ingredient for a successful result on excited states. In the *ab initio* studies presented in this report, we employ large basis sets, CASSCF and CASSCF/MBPT2 calculations to determine the character of and the best description for the  $2p3s$  lowest Rydberg state of pyrazine. In par-

ticular, our calculations address the question of the relative importance for dynamic (MBPT2) and static (CASSCF) correlation for  $n\pi^*$ ,  $\pi\pi^*$ , and Rydberg ( $2p3s$ ) states.

In this paper we present an improved data set for the low lying Rydberg states of the (mono- and di-)azabenzenes and CASSCF and CASSCF/MBPT2 calculations to help analyze the experimental observations.

## II. EXPERIMENTAL APPROACH

Rydberg states for azines lie above  $50\,000\text{ cm}^{-1}$  and are best accessed with current laser techniques by the absorption of two photons to drive the excitation. This implies that high laser power is required. Under conditions of high power, well-focused beams, and the possibility of transition in the vacuum ultraviolet which most medium-sized molecules seem to possess, care must be exercised in assigning observed transitions to particular species. This problem is exacerbated by the high cross section for ionization found for most Rydberg states. As a consequence of these factors, mass resolution and detection of the two photon absorption [ $(2p3s) \leftarrow (2p)^2$ ] by subsequent one-photon ionization [ $(2p)^+ \leftarrow (2p3s)$ ] is greatly preferred, to fluorescence detection techniques.

The supersonic jet/time-of-flight system used in our laboratory previously to study Rydberg states of amines and ethers has been described.<sup>3,9,12</sup> All spectra presented in these studies are obtained through mass-resolved excitation spectroscopy (MRES) monitoring the bare molecule mass channel. A pulsed nozzle is used, at 50 to 80 psig of helium carrier gas, to cool the sample and propel it to the ionization region of the time-of-flight mass spectrometer. The (2+1) MRES are generated by a Nd/YAG pumped dye laser using the dye solutions R640, DCM, R590, Kiton Red, and their mixtures as is appropriate for the observed transitions. The visible dye laser output can be doubled or mixed with Nd/YAG fundamental ( $1.064\text{ }\mu\text{m}$ ), and doubled and mixed to achieve the appropriate wavelengths for the (2+1) resonance-enhanced ionization. Ions are extracted from the ionization region by a focusing structure of 4.0, 3.75, and 0.0 kV grids. Line shapes for the observed transition are measured under conditions of lowest possible power and for no apparent saturation of the transition. The experimental conditions employed in this work yield  $2\text{ cm}^{-1}$  linewidths for dioxane transitions used to calibrate and align the apparatus.

All samples are purchased from Aldrich Chemical Co. and are heated as required in the nozzle to obtain a sample pressure of about 1% of the expansion pressure.

## III. THEORETICAL APPROACH

All calculations presented in this study are performed on an IBM RISC/6000 320H work station with 80 MB of RAM and a total disk storage of 3.6 GM (2.6 GB external and 1 GB internal). The calculations are accomplished with the Hondo 8.5 suite of programs purchased from IBM.<sup>26</sup>

The basis set employed in these calculations is Dunning's contracted double-zeta plus polarization (DZP) set. Additionally,  $3s$ ,  $3p$  Rydberg orbitals are placed on the

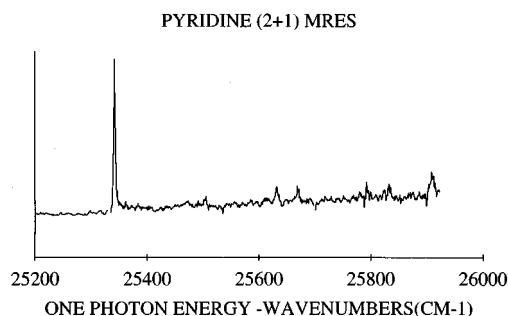


FIG. 1. Two-photon MRES of the Rydberg state transition  $2p3s \leftarrow (2p)^2$  ( ${}^1A_1 \leftarrow {}^1A_1$ ). The vibronic features are weak and assigned in Table I. The gap in the base line just below the two photon origin of pyridine is due to the removal of a transition due to a small amount of dioxane present in the apparatus used to align, calibrate, and test the system. Signal generated in the dioxane mass channel causes a negative feature in the spectrum.

heavy atoms (C and N) for the appropriate calculations. The orbital exponents for these latter orbitals are found in Ref. 27.

The pyrazine calculations are based on  $D_{2h}$  symmetry and three different eigenvalues and eigenvectors are obtained: the ground state (core  $n_1^2 n_2^2 \pi^2 \pi^2 \pi^2$ ); the  $n\pi^*$   ${}^1B_{3u}$  state (core  $n_1^2 n_2, \pi^2 \pi^2 \pi^2 \pi^*$ ); and the  $(2p3s)$  lowest Rydberg state  ${}^1A_{1g}$  (core  $n_1^2, n_2, \pi^2 \pi^2 \pi^2 R_{3s}$ ). The inclusion of atomic  $3s$  and  $3p$  orbitals on the carbon and nitrogen atoms for the ground and  $n\pi^*$  states has very little effect on the energy and wave functions of these states. Polarization functions are found to be important based on results for other amines<sup>8</sup> and based on the numerical results for the present system.

Following the CASSCF calculation, the state energies are computed using many-body perturbation theory to second order (MBPT2). This algorithm accounts for dynamic electron correlation reasonably well within the basis set, geometry, and cost constraints. In particular, the interaction of two simultaneous single excitations is a major contribution to the CASSCF/MP2 calculation.

The Hondo 8.5 CASSCF/MBPT2 algorithm<sup>26</sup> is presently confined to a six electron, six orbital ( $6 \times 6$ ) CASSCF wave function. The pyrazine CASSCF calculations discussed below are ( $6 \times 6$ ) for the ground state ( $3\pi, 3\pi^*$ ), ( $4 \times 5$ ) for the  ${}^1B_{3u}$  state ( $2n, 3\pi^*$ ) and ( $4 \times 6$ ) for the  ${}^1A_{1g}$  Rydberg state ( $2n, 4R$ ). In order to accommodate these various CASSCF wave functions as input to the MBPT2 routine, the convergence criterion is set at  $10^{-3}$ .<sup>26</sup>

## IV. RESULTS AND DISCUSSION

### A. Spectroscopy

#### 1. Pyridine

The two-photon absorption spectrum of the lowest observed Rydberg  $2p3s \leftarrow (2p)^2$  ( ${}^1A_1 \leftarrow {}^1A_1$ ) transition of pyridine is displayed in Fig. 1 and tabulated in Table I. The  $0_0^0$  transition is expanded in Fig. 2 as its shape is fit to both Gaussian and Lorentzian forms. Its shape is approximately Lorentzian, as can be seen in the figure, and is characterized by a full width at half maximum (FWHM) of  $7.45 \text{ cm}^{-1}$ .

TABLE I. Mass resolved excitation spectra (MRES) of the  $[2p3s \leftarrow (2p)^2]$  Rydberg transitions of the mono- and diazabenzenes.

Transition energy ( $\text{cm}^{-1}$ )	Relative shift ( $\text{cm}^{-1}$ )	Assignment <sup>a</sup>
Pyridine		
50 685	0	$0_0^0$
50 946	261	
50 958	273	
51 006	321	
51 263	579	$6a^1$
51 340	655	
51 538	853	
51 560	875	
51 584	899	
51 666	981	$1^1$
51 816	1132	
Pyrazine		
50 835	0	$0_0^0$
51 464	629	$6a^1$
51 827	992	$1^1$
Pyridazine		
53 313	0	$0_0^0$
53 344	31	Hot band
53 385	72	Hot band
53 421	108	Hot band

<sup>a</sup>Vibronic assignments from Ref. 15.

This shape suggests the feature is lifetime (uncertainty) broadened: the lifetime of this state is thus ca. 0.7 ps.

Two totally symmetric vibrations  $6a$  and  $1$  are identified in agreement with previous assignments;  $16a, b^1$  and  $6b^1$  may also be observed, but remain unassigned. Recall that for a two-photon transition, all pyridine vibrational modes can be observed without recourse to vibronic coupling. During the course of this study we searched for hot bands ca.  $1000 \text{ cm}^{-1}$  below the  $0_0^0$  and for higher energy vibrations (greater than  $1100 \text{ cm}^{-1}$ ) to ca.  $1600 \text{ cm}^{-1}$  above the  $0_0^0$  but found no reproducible features occurring in the pyridine or lower mass channels. The pyridine ionization threshold is ca.  $9.27 \text{ eV}$  (ca.  $74\,740 \text{ cm}^{-1}$ );<sup>15</sup> three times the laser energy ( $2+1$  ionization) is  $76\,027.5 \text{ cm}^{-1}$  which should not be enough energy to cause significant pyridine fragmentation. Since no signals are observed in lower mass channels, we can assume

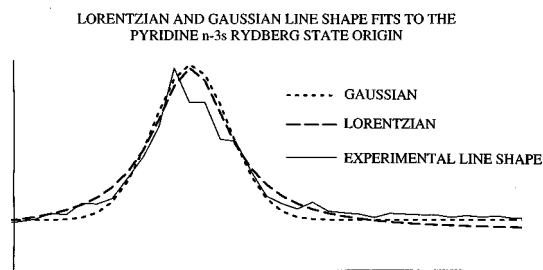


FIG. 2. Gaussian and Lorentzian fits to the pyridine ( $n-3s$ ) Rydberg state origin transition are depicted. The fit is approximately Lorentzian with lifetime broadening characterized by a 0.7 ps lifetime for the Rydberg state. The quality of the fit is limited by the poor signal-to-noise ratio for this weak transition.

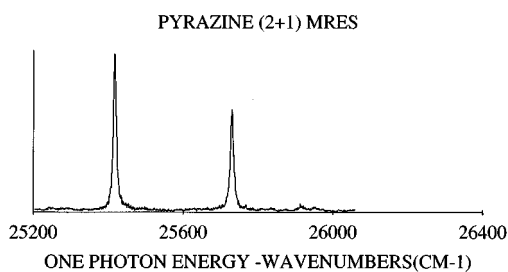


FIG. 3. Two-photon MRES of the lowest energy Rydberg state of pyrazine. The features are assigned in Table I.

that the employed intensity is insufficient to cause further photoabsorption in the pyridine ion that leads to parent ion fragmentation.

To the best of our knowledge this is the only cold, mass-resolved excitation spectrum obtained for the  ${}^1A_1(2p3s)$  Rydberg state of pyridine.

## 2. Pyrazine

The two-photon  $2p3s \leftarrow 2p^2$  Rydberg spectrum ( ${}^1Ag \leftarrow {}^1Ag$ ) of pyrazine is presented in Fig. 3 and Table I. Figure 4 shows an expanded view of the  $0_0^0$  and its fit to Lorentzian and Gaussian line shapes. The associated lifetime of the excited state for the Lorentzian shape is ca. 0.3 ps, corresponding to a ca.  $15 \text{ cm}^{-1}$  FWHM. The  $6a^1$  and  $1^1$  vibrations can be identified in this spectrum. The spectra are observed in the pyrazine mass channel only. Again the (2+1)-photon process should not cause pyrazine fragmentation because its ionization threshold is ca.  $74\,350 \text{ cm}^{-1}$ , about  $2000 \text{ cm}^{-1}$  below the three photon absorption energy.

These spectra appear to be the only ones obtained for cold molecules and with mass resolution.

## 3. Pyrimidine

The  $2p3s \leftarrow (2p)^2$  ( ${}^1B_2 \leftarrow {}^1A$ ) Rydberg spectrum of pyrimidine is not observed in these experiments. The system alignment is monitored during the search with a small amount of dioxane, which also absorbs in this region<sup>9</sup> and the nozzle is heated to  $70^\circ\text{C}$  to ensure that sufficient pyrimidine is present in the expansion gas. The laser scan range is from  $24\,500$  to  $26\,000 \text{ cm}^{-1}$  which corresponds the two photon transition ranges of  $49\,000$  to  $52\,000 \text{ cm}^{-1}$ . Lower

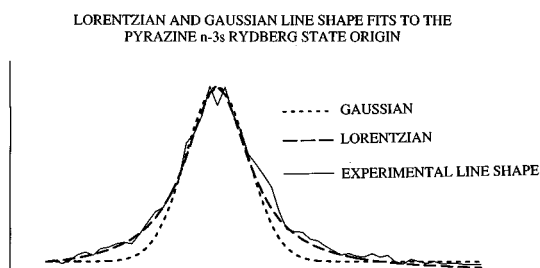


FIG. 4. Gaussian and Lorentzian fits to the pyrazine ( $n-3s$ ) Rydberg state origin transition are depicted. A Lorentzian shape is the better fit and the Rydberg state thus has a characteristic lifetime of about 0.3 ps.

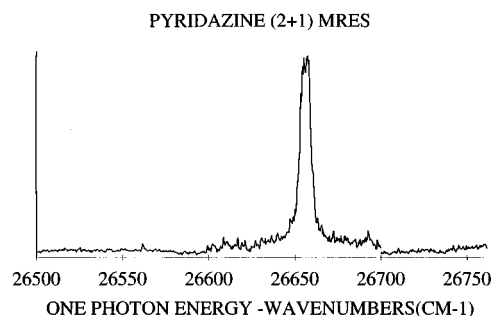


FIG. 5. Two-photon MRES of pyridazine from about  $53\,000$  to  $53\,400 \text{ cm}^{-1}$  is shown. One can suggest that it is a Rydberg state because of its relative intensity and linewidth. A small gap in the spectrum is due to the removal of a dioxane lineup feature which causes a negative peak in the pyridazine mass channel.

mass channels are also monitored for fragment related signals. No transitions are observed in any appropriate mass channel that can be attributed to pyrimidine in this range.

## 4. Pyridazine

The main feature observed for pyridazine in this work lies at  $53\,313 \text{ cm}^{-1}$  and is shown in Fig. 5. Table I lists the transition origin and a few observed hot bands for this molecule. The line shape is fit to both a Gaussian and a Lorentzian as presented in Fig. 6. The Lorentzian line shape is apparently the more appropriate and corresponds to a  $15.2 \text{ cm}^{-1}$  FWHM and a Rydberg state decay time of 0.4 ps. This transition is identified by Ref. 15 as involving an excited triplet state. Considering its intensity and similarity to the other observed features reported above, we consider this possibility unlikely.

Additionally we observe no features at previously reported lower energies,  $51\,503 \text{ cm}^{-1}$  (Ref. 15) and  $47\,565 \text{ cm}^{-1}$  (Ref. 16) with detection in the pyridazine mass channels.

As to the actual assignment of the observed transition, one can only suggest that it is a Rydberg state because of its linewidth and relative intensity with respect to background in ionization mass-resolved detected spectra. Rydberg states are suggested to have much larger cross sections for ionization than do valence states.<sup>5</sup> The most certain approach to this assignment given the relatively low pyridazine symmetry

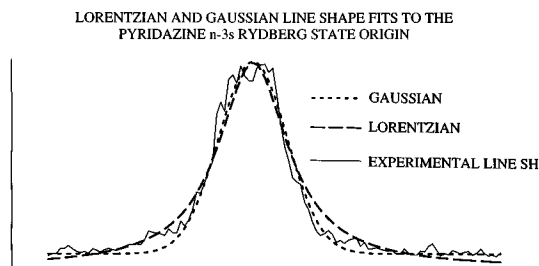


FIG. 6. Gaussian and Lorentzian fits to the  $n-3s$  Rydberg state origin transition of pyridazine. The Rydberg state lifetime associated with the Lorentzian fit is approximately 0.4 ps. Noise on this weak signal limits the quality of the fit.

TABLE II. Results of RHF, CASSCF, and CASSCF/MBPT2 calculations for pyrazine. The Dunning's double-zeta valence plus polarization (DZP) contracted basis set is used in all cases (Ref. 27). Rydberg orbitals are included and excluded as noted.

Calculation type and state	Energy (3s,3p) (Hartrees)	Energy (no 3s, 3p) (Hartrees)	Transition energy (cm <sup>-1</sup> )		Observed
			S <sub>0</sub> with 3s, 3p	S <sub>0</sub> without 3s, 3p	
RHF (A <sub>1g</sub> ,S <sub>0</sub> )	-262.731 6958	-262.730 0593	...	...	
CASSCF (π, π*, S <sub>0</sub> ) <sup>a</sup>	-262.814 3244	-262.812 6942	...	...	
CASSCF (n, π*, <sup>1</sup> B <sub>3u</sub> , S <sub>1</sub> ) <sup>b</sup>	-262.643 8885	...	37 406 (CASSCF)	37 048 (CASSCF)	30 875 <sup>d</sup>
CASSCF <sup>1</sup> A <sub>1g</sub> (2p3s) (n, 3s, 3p)	-262.492 3441	N/A	70 666 (CASSCF)	70 308 (CASSCF)	50 835
			53 531 (RHF)	52 172 (RHF)	
CASSCF+MP2 <sup>c</sup> (π, π*, S <sub>0</sub> ) <sup>a</sup>	-263.588 6539		...	...	
CASSCF+MP2 (n, π*, <sup>1</sup> B <sub>3u</sub> , S <sub>1</sub> ) <sup>b</sup>	-263.474 3358		25 089	...	
CASSCF+MP2 <sup>1</sup> A <sub>1g</sub> (2p3s) (n, 3s, 3p)	-263.366 5997		48 735	...	

<sup>a</sup>The orbitals π and π\* indicate which orbitals are included in the active space of the CASSCF calculation. This is a ground state calculation that includes valence orbitals as part of the active space.

<sup>b</sup>The orbitals n and π\* indicate which orbitals are included in the active space of the CASSCF calculation.

<sup>c</sup>These calculations utilized one geometry point and no geometry optimization. The input geometry was the corresponding CASSCF output geometry for all three CASSCF+MP2 calculations.

<sup>d</sup>See Ref. 15.

would be through high level *ab initio* calculations. The transition could be associated with either a 3s or 3p Rydberg state.

## B. Calculations—Pyrazine

In order to help explain the nature and spatial distribution of the low lying Rydberg states of the azines, we have performed a series of *ab initio* calculations on the ground state, *nπ\** first excited singlet state (<sup>1</sup>B<sub>3u</sub>), and lowest Rydberg state (2p3s, <sup>1</sup>A<sub>1g</sub>) of pyrazine (*D*<sub>2h</sub> symmetry). If this calculation were to give satisfactory results for the transition energies involved (ca. 30 000 cm<sup>-1</sup> <sup>1</sup>B<sub>3u</sub> ← <sup>1</sup>A<sub>1g</sub>, ca. 50 000 cm<sup>-1</sup> <sup>1</sup>A<sub>1g</sub>(R<sub>3s</sub>) ← <sup>1</sup>A<sub>1g</sub>) we could then proceed to apply similar techniques to the other systems. The pyrazine excited states are clearly the best documented and well understood both experimentally and theoretically. Pyrazine's higher symmetry is, of course, partly responsible for this situation.

The results of such calculations are given in Table II and are described and discussed below. In order to obtain good transition energies for any species, one must be certain to generate ground and excited state energies at the same level of approximation and with roughly equal inclusion of static and dynamic correlation contributions. In order to ensure convergence for the ground state complete active space self-consistent-field (CASSCF) calculation, the *n* electrons and orbitals are frozen along with the core. A converged result obtains, with or without Rydberg orbitals, for a (6×6) (π, π\*) CASSCF calculation of the ground state. As can be seen from Table II the inclusion of Rydberg 3s, 3p orbitals has little effect on the ground state energy (~360 cm<sup>-1</sup>); the 3s

and 3p orbitals make very little contribution to the occupied *n* and π molecular orbitals. This holds true for both RHF and CASSCF levels.

To test the calculational algorithm on a well-known state, the *nπ\** <sup>1</sup>B<sub>3u</sub> first excited singlet state of pyrazine is calculated. Again the calculation is done with and without Rydberg orbitals with little observed difference in energy or wave function. In both cases two *n* orbitals (A<sub>g</sub>, B<sub>1u</sub>), three π orbitals (B<sub>3u</sub>, B<sub>2g</sub>, B<sub>1g</sub>), and three π\* orbitals (B<sub>3u</sub>, A<sub>u</sub>, B<sub>2g</sub>) are used in the CASSCF calculation (10×8). The transition energy for the <sup>1</sup>B<sub>3u</sub>*nπ\** ← <sup>1</sup>A<sub>g</sub> *n*<sup>2</sup> transition is 37 406 cm<sup>-1</sup>, which is 6531 cm<sup>-1</sup> (0.81 eV) higher than observed. While this is quite high in general, the result is not unexpected for a totally delocalized calculation and is consistent with other molecular orbital results at comparable levels.<sup>11,17,18,21</sup> Polarization functions (*d* functions on C and N and *p* functions on H) also have no major effect on the ground and excited state energies.

To test this approach on the Rydberg states of pyrazine, two different CASSCF calculations for the <sup>1</sup>A<sub>g</sub>(3s2p) lowest Rydberg state are performed. The first freezes the π and π\* orbitals and includes both *n* orbitals and three A<sub>g</sub> Rydberg virtual orbitals (large 3s coefficients) from the *nπ\** <sup>1</sup>B<sub>3u</sub> CASSCF calculation. The second CASSCF calculation includes seven virtual orbitals of Rydberg character: four A<sub>g</sub>, one B<sub>2g</sub>, one B<sub>3u</sub>, and one A<sub>u</sub>. The second CASSCF calculation is characterized by a four electron, nine orbital active space. Both calculations give very similar results: the four electron, nine orbital results are presented in Table II. The energy for the transition <sup>1</sup>A<sub>1g</sub> ← <sup>1</sup>A<sub>1g</sub> is roughly 20 000 cm<sup>-1</sup>

too high at this level of theory. Apparently, inclusion of  $\sigma\sigma^*$  excitations and dynamic electron correlation is required to lower the energy of the Rydberg state; thus the CASSCF active space would need to be increased significantly or special states would need to be included in the active space in order to account for these localization/dynamic correlation effects. CI singles and doubles multiconfiguration self-consistent-field (CISD MCSCF) calculations show that many virtual orbitals contribute to the Rydberg state description.<sup>11</sup>

Some of the dynamic correlation missing from the CASSCF excited states can be included using a CASSCF plus second-order many-body perturbation theory (MBPT2) algorithm. The Hondo 8.5 programs has the Davidson approach<sup>28</sup> which can approximate extensive multireference CI calculations. These calculations are performed for one single geometry as calculated at the CASSCF level. Table II presents those results. As can be seen from this table, the transition energies for both  $n\pi^*$  and ( $3s2p$ ) Rydberg states are greatly improved. These transition energies demonstrate that dynamic correlation and intensive CI will generate a reasonable description of the electronic structure of the azabenzenes.

More extensive calculations that would include a new geometry search based on the CASSCF wave function in conjunction with the MBPT2 algorithm would probably generate more satisfactory transition energies; nonetheless, these results adequately demonstrate the need for extensive electron correlation in order to model the azabenzene states in general.

Table III shows the geometry of pyrazine in its ground,  $n\pi^*$  and Rydberg excited states at the CASSCF level. As expected, the Rydberg excitation in particular changes the shape of the pyrazine molecule around the C–N–C site. Since the lone pair has been delocalized, the C–N–C angle can open considerably. The excited states of pyrazine take on a quinoidal-like structure in which the two nitrogen atoms move toward the center of mass to open the C–N–C angles from 116° to 125°.

These results are not dissimilar from those obtained for azabicyclooctane<sup>11</sup> and methylamine.<sup>8</sup> In those instances, Rydberg and other excited state CASSCF/CI calculations give good results for transition energies. They also suggest a more open C–N–H and C–N–C angle and a delocalized Rydberg wave function.

## V. CONCLUSIONS

The experimental spectra for the lowest Rydberg states of the azabenzenes are reported for expansion-cooled samples. Transitions are confirmed for pyridine and pyrazine but not pyrimidine and pyridazine. Linewidth data suggest that the excited states are short lived. The signals of all of the low lying Rydberg states of azabenzenes in this work are weak and are apparently lifetime limited with respect to nanosecond laser excitation and detection. Given the short lifetimes of these Rydberg states a pulsed laser with a temporal bandwidth of 100 fs would in principle yield a larger ionization signal.

*Ab initio* CASSCF and CASSCF/MBPT2 calculations have been carried out for pyrazine which show that dynamic

TABLE III. Geometry of pyrazine in different electronic states. The calculations are described in the text.

State and calculation type	Angles	Distances (Bohr)		
		N–C	C–H	C–C
Ground state <sup>a</sup> CASSCF	C–N–C angle	2.519	2.031	2.647
	116.075			
	N–C–C angle			
	121.963			
	N–C–H angle			
	117.223			
$n, \pi^*$ Excited state CASSCF	C–C–H angle			
	120.815			
	C–N–C angle	2.564	2.026	2.622
	119.491			
	N–C–C angle			
	120.257			
Rydberg state <sup>c</sup> CASSCF	N–C–H angle			
	119.465			
	C–C–H angle			
	120.281			
	C–N–C angle	2.438	2.030	2.694
	125.070			
	N–C–C angle			
	117.466			
	N–C–H angle			
	122.200			
	C–C–H angle			
	120.335			

<sup>a</sup>CASSCF (six electrons, six orbitals) with Rydberg.

<sup>b</sup> $n, \pi^*$  CASSCF (ten electrons, eight orbitals) with Rydberg orbitals.

<sup>c</sup> $n, 3s, 3p$  CASSCF (four electrons, nine orbitals).

electron correlations at the MBPT2 level are important for the excited states. Extensive configuration interaction is required to obtain good energy values for  $n\pi^*$  and Rydberg transitions.

## ACKNOWLEDGMENTS

The authors wish to thank Professor A. K. Rappé for his many discussions and helpful comments concerning the calculations presented in the report. The work was supported by the USARO.

<sup>1</sup>(a) See for example the most recent review by K. Müller-Dethlefs, O. Doppler, and T. G. Wright, *Chem. Rev.* **94**, 1845 (1994); (b) K. Müller-Dethlefs and E. W. Schlag, *Annu. Rev. Phys. Chem.* **42**, 109 (1991).

<sup>2</sup>(a) B. M. Dobratz, *LLNL Explosives Handbook* (NTIS, 1982), DE85-015961, revised; (b) G. F. Adams and R. W. Shaw, Jr., *Annu. Rev. Phys. Chem.* **43**, 311 (1992); (c) M. J. McQuaid, A. W. Miziolek, R. C. Sausa, and C. N. Merrow, *J. Phys. Chem.* **95**, 2713 (1991).

<sup>3</sup>Q. Y. Shang, P. O. Moreno, and E. R. Bernstein, *J. Am. Chem. Soc.* **116**, 311 (1994).

<sup>4</sup>Q. Y. Shang, C. F. Dion, and E. R. Bernstein, *J. Chem. Phys.* **101**, 118 (1994).

<sup>5</sup>(a) M. B. Robin, *Higher Excited States of Polyatomic Molecules* (Academic, New York, 1974), Vol. 1; (b) Note, however, that the seminal work of Mulliken [R. S. Mulliken, *J. Chem. Phys.* **3**, 506 (1935)] does indeed take a more balanced approach. Also the early work of Lawson *et al.* on

- acetone [M. Lawson and A. B. F. Duncan, *J. Chem. Phys.* **12**, 329 (1944)] demonstrates this through spectral analysis.
- <sup>6</sup>Q. Y. Shang, P. O. Moreno, R. Disselkamp, and E. R. Bernstein, *J. Chem. Phys.* **98**, 3703 (1993).
- <sup>7</sup>Q. Y. Shang and E. R. Bernstein, *J. Chem. Phys.* **100**, 8625 (1994).
- <sup>8</sup>D. P. Taylor and E. R. Bernstein (in preparation).
- <sup>9</sup>P. O. Moreno, Q. Y. Shang, and E. R. Bernstein, *J. Chem. Phys.* **97**, 2869 (1992).
- <sup>10</sup>D. P. Taylor and E. R. Bernstein, *J. Chem. Phys.* (to be published).
- <sup>11</sup>R. Disselkamp, Q. Y. Shang, and E. R. Bernstein, *J. Phys. Chem.* **99**, 7227 (1995).
- <sup>12</sup>(a) K. Law, M. Schauer, and E. R. Bernstein, *J. Chem. Phys.* **80**, 207 (1984); (b) For a general reference, see D. H. Levy, *Adv. Chem. Phys.* **47**, 323 (1981).
- <sup>13</sup>V. Vaida, *Acc. Chem. Res.* **19**, 114 (1986).
- <sup>14</sup>D. P. Taylor and C. F. Dion (unpublished results).
- <sup>15</sup>K. K. Innes, I. G. Ross, and W. R. Moomaw, *J. Mol. Spectrosc.* **132**, 492 (1988).
- <sup>16</sup>J. G. Philis, *J. Mol. Spectrosc.* **155**, 215 (1992).
- <sup>17</sup>W. R. Wadt and W. A. Goddard III, *J. Am. Chem. Soc.* **97**, 2034 (1975).
- <sup>18</sup>W. R. Wadt, W. A. Goddard III, and T. H. Dunning, Jr., *J. Chem. Phys.* **65**, 1583 (1976).
- <sup>19</sup>J. C. Ellenbogen, D. Feller, and E. R. Davidson, *J. Phys. Chem.* **86**, 1583 (1982).
- <sup>20</sup>I. C. Walker and M. H. Palmer, *Chem. Phys.* **153**, 169 (1991).
- <sup>21</sup>M. P. Fulsher, K. Anderson, and B. O. Roos, *J. Phys. Chem.* **96**, 9204 (1992).
- <sup>22</sup>R. J. Bartlett, *Annu. Rev. Phys. Chem.* **32**, 259 (1981).
- <sup>23</sup>I. N. Levine, *Quantum Chemistry* (Prentice-Hall, Englewood Cliffs, NJ, 1991), 4th ed.
- <sup>24</sup>M. H. Palmer, I. C. Walker, M. F. Guest, and A. Hopkirk, *Chem. Phys.* **147**, 19 (1990).
- <sup>25</sup>I. C. Walker, M. H. Palmer, and A. Hopkirk, *Chem. Phys.* **141**, 365 (1989).
- <sup>26</sup>M. Dupuis, F. Johnston, and A. Marquez, *HONDO 8.5 from CHEM-Station*, (1994) IBM Corporation, Neighborhood Road, Kingston, NY, 12401.
- <sup>27</sup>*Methods of Electronic Structure Theory*, edited by H. F. Schaefer (Plenum, New York, 1977), Vol. III.
- <sup>28</sup>P. M. Kozlowski and E. R. Davidson, *J. Chem. Phys.* **100**, 3672 (1994).